Desalination and Water Treatment
www.deswater.com

doi: 10.5004/dwt.2019.23331

138 (2019) 200–207
January

Active control optimization for anaerobic digestion processes

Bui Duc Hong Phuc[a], Sam-Sang You[b,*], Nguyen Ngoc Nam[b], Hwan-Seong Kim[c]

[a]*School of Intelligent Mechatronics Engineering, Sejong University, Gwangjin-gu, Seoul 143-747, South Korea, Tel. +82 2 6935 2440; email: buidhp@sejong.ac.kr*
[b]*Division of Mechanical Engineering, Korea Maritime and Ocean University, Yeongdo-gu, Busan 606-791, South Korea, Tel. +82 51 410 4366; emails: ssyou@kmou.ac.kr (S.-S. You), nnnam@kmou.ac.kr (N.N. Nam)*
[c]*Department of Logistics, Korea Maritime and Ocean University, Yeongdo-gu, Busan 606-791, South Korea, Tel. +82 51 410 2409; email: kimhs@kmou.ac.kr*

Received 8 June 2018; Accepted 19 October 2018

ABSTRACT

Anaerobic digestion is currently the most popular process for renewable energy by collecting biogas from organic degradable materials. The main barriers include significant changes in the input composition, external disturbance, and the high cost and complexity of the analyzing system. In this paper, after some nonlinear analyses, the observer-based robust controller is designed for the linearized system to replace the limitations of conventional controllers dealing with those problems. The chemical oxygen demand concentration and dilution rate are selected as controlled and manipulated variables, respectively. The volatile fatty acid is the system state to be estimated, providing that there is no sensor to analyze this composition. The simulation results show that the achieved controller can regulate chemical oxygen demand concentration under large disturbances and plant uncertainties as well as can exactly estimate the volatile fatty acid. Applying this approach can help to increase the robustness of anaerobic digestion processes and to reduce the investment cost by replacing some expensive sensors.

Keywords: Anaerobic digestion; Chemical oxygen demand; Observer; Robust control; Volatile fatty acid

1. Introduction

Anaerobic digestion (AD) is the most popular process for renewable energy production due to its ability to convert organic degradable materials into biogas. The composition of the achieved gas includes 60%–65% methane (CH_4), 30%–35% carbon dioxide (CO_2), and a small part of H_2, N_2, H_2S, and H_2O. The most valuable gas collected is methane, which can be used as hydrocarbon fuel for combustion in combined heat and power plants. The biogas is extracted while the remainder is dried and used as fertilizer or residual soil-like material. The process occurs in the environment without oxygen, called anaerobic dioxide.

Common substrates in AD are wastewater, manure, crops, and organic fractions of municipal solid waste [1]. Nowadays, AD is mainly used for wastewater treatment [2]. In the activated sludge process (ASP) for wastewater treatment, a mass of microorganisms is cultivated to break down organic matter into carbon dioxide, water, and other inorganic compounds. The waste-activated sludge rejected from the process is not safe for the environment, but it needs further treatment. Therefore, AD is often built with ASP in one wastewater treatment plant to digest the wasted sludge and collect valuable biogas as well. The complete combination of ASP and AD is illustrated as in Fig. 1.

The AD process includes a reactor, a mixing pump, a heat exchanger, a dilution system, and an input pump. The detailed structure of an AD process is described in Fig. 2.

Controlled inputs or manipulated variables in the automatic control of AD process should have quick and significant

* Corresponding author.

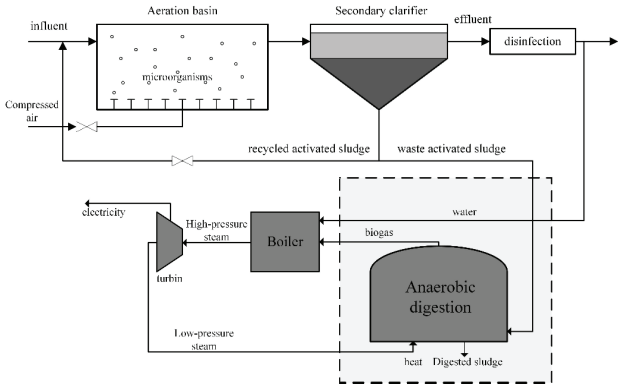

Fig. 1. Wastewater treatment system with activated sludge and anaerobic digestion process.

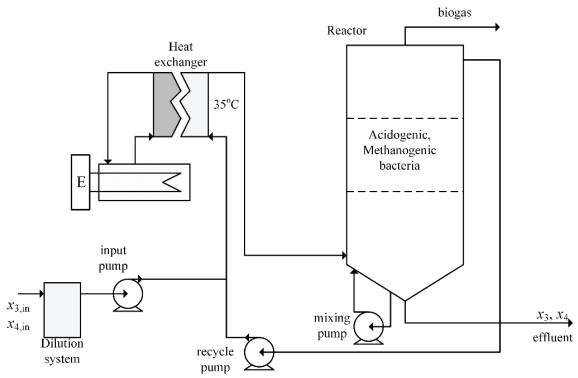

Fig. 2. Schematic diagram of an anaerobic digestion system.

impacts on the system performance. Depending on the applications in AD process, the control variables include methane flow rate, chemical oxygen demand (COD) concentration in the effluent, or volatile fatty acid (VFA) while feeding rate is the most common manipulated variable. By using feeding rate as manipulate variables, it is possible to simultaneously regulate the retention time and organic loading rate, allowing microbial communities in the system to adapt to some disturbances. The feeding rate can be represented by dilution rate, which is the ratio between the flow rate of the substrate and the liquid volume of the digester.

The controlling of an AD process is very challenging due to the following problems: (i) the variations of wastewater in quantity and composition, (ii) biomass activity changes under the influence of internal and external factors, (iii) lack of adequate sensor for online measurements, and (iv) parametric uncertainties [2].

For industrial scale AD plants, basic parameters such as pH, temperature, mixed liquor level, gas pressure, mixed liquor and biogas flow rate should be monitored online for effective wastewater treatment. In fact, an online monitoring system was not implemented in many industrial plants. In a study by Spanjers and Lier [3], only 10% of 400 industrial scale AD plants worldwide are equipped with online analysis of COD, TOC, VFAs, alkalinity, and biogas composition. It could be explained by the complexity of its operations and maintenances of the advanced analysers or sensors. Additionally, high capital and operation costs of these state-of-the-art devices make it economically unattractive for AD operators to embrace the technology.

For the wastewater treatment plants with online monitoring systems, the control system was simple, time-based, and equipped with on/off controllers. Many control methods have been proposed in recent years for AD processes. They could be simple ones such as feedback on/off control, proportional-integral-derivative or higher ones such as adaptive, fuzzy, and neural network controllers. However, conventional control methods have not been able to cope with the inherent difficulties of AD processes [4,5]. Moreover, classical control methods generally give *unsatisfactory performances* when AD processes are subjected to large disturbances or significant set-point changes [2]. Some advanced robust controllers have been designed to regulate AD processes which ensure some robustness [2,5].

In this paper, a robust loop-shaping controller is designed on a robust observer to control the COD concentration under influent uncertainty as well as disturbances, and to estimate VFA, in the case of no equipment to measure this parameter. The success of this kind of controller can contribute much to the development of AD plants such as improving the stability and robustness for AD systems under uncertainties and disturbances, and reducing the investment costs by replacing some expensive sensors and complicate analysers.

2. Dynamical model of AD

In the last three decades, many dynamical models have been developed to provide better understanding and prediction of AD process, such as in the studies by Hill [6], Bernard et al. [7], Batstone et al. [8], and Siegrist et al. [9]. Among the models, Bernard et al.'s [7] study has been used widely for control synthesis purpose. This is a sixth-order model including the mass balances equations of acidogenic and methanogenic biomass, organic, and VFAs substrates, alkalinity, and total inorganic carbon. In order to design the observer-based robust controller, the reduced fourth-order model relating the dynamics of acidogenic, methanogenic bacteria, COD, and VFAs [2,10] is chosen as follows:

$$\dot{x}_1 = (\mu_1(x_3) - \alpha D)x_1 \tag{1}$$

$$\dot{x}_2 = (\mu_2(x_4) - \alpha D)x_2 \tag{2}$$

$$\dot{x}_3 = (x_{3,in} - x_3)D - k_1\mu_1(x_3)x_1 \tag{3}$$

$$\dot{x}_4 = (x_{4,in} - x_4)D + k_2\mu_1(x_3)x_1 - k_3\mu_2(x_4)x_2 \tag{4}$$

$$\mu_1(x_3) = \mu_{1\max}\frac{x_3}{x_3 + K_{s1}} \tag{5}$$

$$\mu_2(x_4) = \mu_{2\max}\frac{x_4}{(x_4)^2 / K_{I2} + x_4 + K_{s2}} \tag{6}$$

where x_1 represents the acidogenic bacteria concentration (g/L); x_2 is the methanogenic bacteria concentration (g/L);

x_3 the COD (g/L); x_4 the VFA (mmol/L); $x_{3,in}$ and $x_{4,in}$ denote the inlet concentrations; and $\mu_1(x_3)$ and $\mu_2(x_4)$ are the growth rates of acidogenic and methanogenic bacteria, respectively. α is the parameter reflecting the process heterogeneity: α = 0 corresponds to an ideal fixed-bed reactor, whereas α = 1 indicates an ideal continuous stirred-tank reactor. All the parameters are given in Table 1.

As described in Eqs. (1)–(6), the dynamical model is highly nonlinear and very demanding to be controlled due to the interconnection between the state variables, uncertainties, and disturbances. There have been some works analyzing the nonlinear behaviours of the AD systems such as in the study by Sbarciog et al. [10]. The paper considered some possible major cases with different values of dilution, influent COD, and VFA. These cases show equilibrium points at different working conditions. Most of the equilibrium points represent the washout of both acidogenic and methanogenic bacteria, or one of them, while some points indicate the coexistence of them. The coexistence is important and necessary for good operating conditions of the AD system because the bacteria's role is to convert organic components into biogas. The washout of the bacteria must be avoided to ensure the conversion of the substrates. Otherwise, there will be accumulations of COD and VFA in the reactor.

Table 1
Model parameters of AD process

Parameter	Value
α	1
k_1	42.14
k_2, mmol/g	116.5
k_3, mmol/g	268
μ_{1max}, h^{-1}	1.2
μ_{2max}, h^{-1}	0.74
K_{S1}, g/L	7.1
K_{S2}, mmol/L	9.28
K_{I2}, mmol/L	256
$x_{3,in}$, g/L	0–50
$x_{4,in}$, mmol/L	0–200

It is known that the parameter whose value has the most significant variation is $x_{3,in}$ (influent COD). In Fig. 3, the nonlinear behaviour is analyzed at D = 0.5, $x_{4,in}$ = 30 mmol/L, with different values of $x_{3,in.}$

The simulation shows that at $x_{3'in}$ = 30 g/L, the system has some equilibrium points indicating the coexistence of the bacteria. At $x_{3'in}$ = 10.691 g/L, the system converges to one coexistence point, and at $x_{3'in}$ = 5.1646 g/L, the system behaviour converges to 0, indicating the total washout of both bacteria. Note that at any value of $x_{3'in}$, the initial point without one of the bacteria will lead to the equilibrium point at 0. This nonlinear analysis proves that influent parameter variation can totally change system behaviour and can deeply affect the operation of the system. However, by applying some control algorithms to control the dilution, the total washout of the bacteria can be avoided, and the coexistence of the biomass can be robustly maintained.

From the nonlinear models in Eqs. (1)–(6), a linear model is realized so that the robust control algorithm can be applied. The linearization is performed near an equilibrium point where there is a coexistence of the biomass, such as at $x_{4,in}$ = 30 mmol/L and $x_{3'in}$ = 30 g/L. By applying a Taylor expansion of the differential equations and Jacobian matrix, a linear state-space model can be achieved whose components

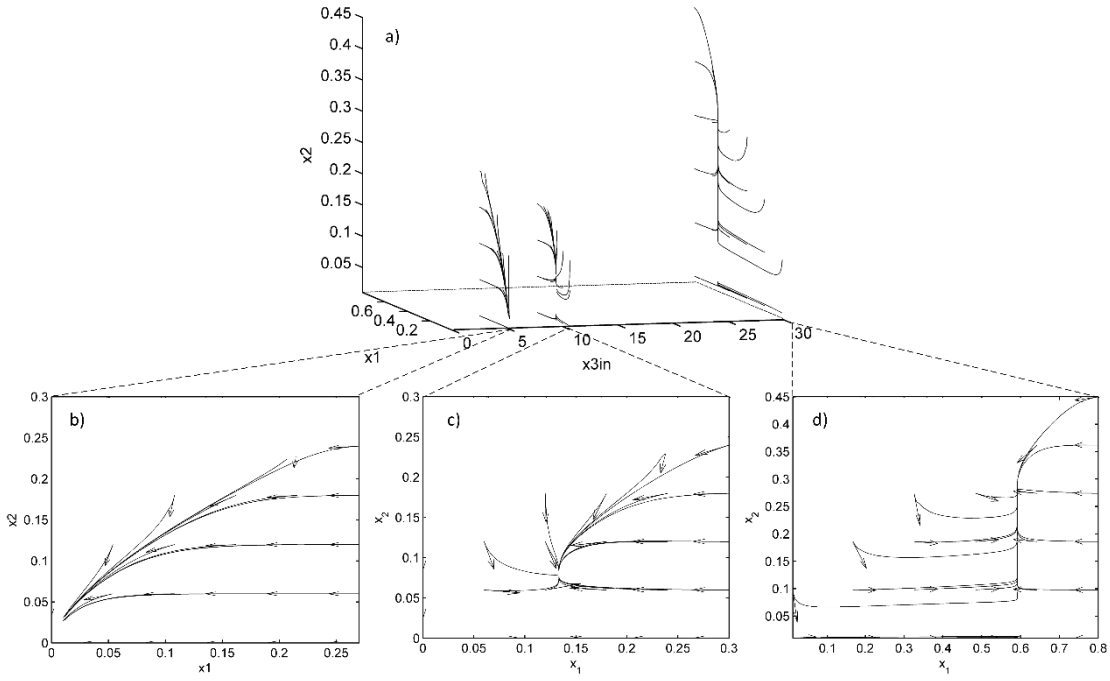

Fig. 3. Phase portrait of the nonlinear system at different values of influent COD concentration ($x_{3'in}$): (a) global 3D graph of phase portraits; (b) phase portrait at $x_{3'in}$ = 5.1646 g/L; (c) phase portrait at $x_{3'in}$ = 10.691 g/L; and (d) phase portrait at $x_{3'in}$ = 30 g/L.

matrices are given in Appendix A. The state space then will be converted to a transfer function *G*, which will be used further in the control design process. The transfer function is also given in Appendix A. Note that in the linearized system, the manipulated variable is the dilution *D*, which is performed by adding water to influent sludge, the controlled variable is the COD concentration, and the observed state is VFA concentration.

3. Robust controller design

3.1. H∞ loop-shaping controller

In the robust control approach, the control objective is to stabilize not only the nominal plant *G* but also the set of perturbed plant G_p using a dynamic feedback controller *K*. A loop-shaping technique allows the system designer to specify closed-loop objectives by shaping the loop gains of the control system. If the functions W_1 and W_2 are selected as the pre- and post-compensators, respectively, then the shaped plant as illustrated in Fig. 4 with its coprime factorization is given as follows:

$$G_s(s) = W_2(s)G(s)W_1(s) = M_s^{-1}N_s \tag{7}$$

where W_2 is selected as the identity matrix, and W_1 is a diagonal matrix which is used to shape the frequency response of the nominal model and to specify the closed-loop behaviours.

Typically, the loop gains have to be large at low frequencies for good disturbance rejection at both the input and output of the plant, and small at high frequencies for noise rejection. In addition, the desired opened-loop shapes are chosen to be approximately –20 dB/decade roll-off around the crossover frequency to achieve desired robust stability, gain and phase margins, overshoot, and damping.

The shaping function W_1 is chosen as follows:

$$W_1(s) = \left(\frac{s+20}{s+10^{-3}}\right)^2 \tag{8}$$

The frequency response of the shaped plant is described in Fig. 5. Because the wastewater plant operates in very low-frequency ranges, it is shaped only in this frequency to eliminate the effect of disturbance.

3.2. Coprime factor uncertainty

Robust stability bounds regarding the H_∞ norm are conservative if there are many perturbation blocks at different positions in the AD system. To get tighter bounds, the uncertainties are described using the left coprime factorization (LCF) [11] as depicted in the dashed rectangle in Fig. 6. In this structure, uncertainty blocks enter and exit from the same position. Therefore, they can be combined to form a full perturbation block.

Note that in the coprime factor uncertainty description in Fig. 6, there is no weighting block. The description is based on addictive perturbations to the LCF. The robust stabilization problem is to stabilize the set of perturbed plants as follows:

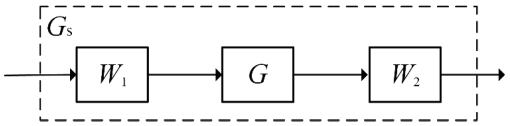

Fig. 4. Shaped open-loop system.

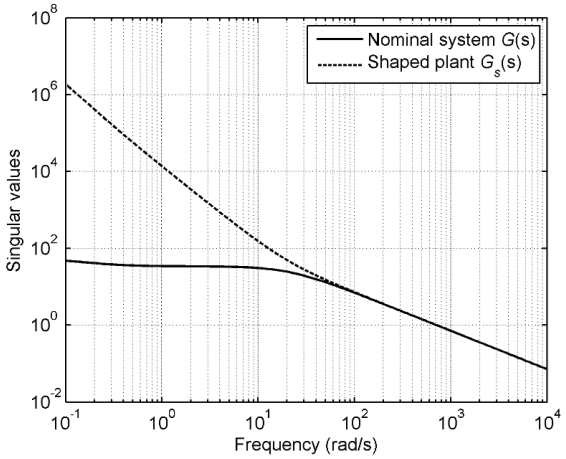

Fig. 5. Singular value plot of nominal system and shaped loop gain.

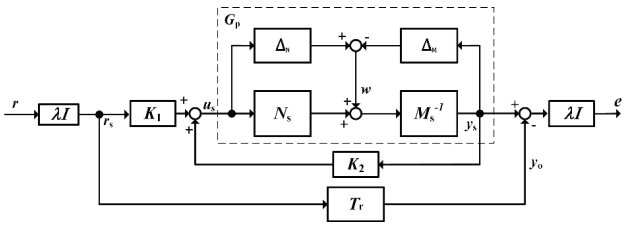

Fig. 6. 2-DOF control configuration with coprime perturbation.

$$G_p = (M_s + \Delta_M)^{-1}(N_s + \Delta_N), \qquad \left\| \begin{bmatrix} \Delta_N & -\Delta_M \end{bmatrix} \right\|_\infty \le \varepsilon \tag{9}$$

where $M_s^{-1}N_s = G_s$ is the normalized LCF of the shaped plant, and ε is the stability margin with M_s, N_s, Δ_M, and $\Delta_N \in \Re H_\infty$.

3.3. Control synthesis

For stringent tracking problem in the AD system, one-degree-of-freedom controller will not be sufficient to meet both requirements for reference tracking and disturbance rejection. Hence, a dynamic 2-DOF (degree-of-freedom) controller is proposed using the approach in the study by Hoyle et al. [12]. The 2-DOF feedback control scheme is depicted schematically in Fig. 6.

The 2-DOF controller includes the feedback part K_2 that satisfies the requirements of internal and robust stability, disturbance rejection, measurement noise attenuation, and sensitivity minimization; and the pre-compensator K_1 that optimizes the response of the overall system to the command input such that the output of the system would be close to that of a chosen ideal system T_r. More explicitly, T_r represents

some desired closed-loop transfer functions between reference input and output. For this specific application, the scaling value l is chosen as 1.

The shaped plant is supposed to be strictly proper, with a stabilizable and detectable state-space realization.

$$G_s = \left[\begin{array}{c|c} A_s & B_s \\ \hline C_s & 0 \end{array}\right] \tag{10}$$

And the desired (reference) closed-loop transfer function is given as follows:

$$T_r = \left[\begin{array}{c|c} A_r & B_r \\ \hline C_r & 0 \end{array}\right] \tag{11}$$

To form the standard control configuration, a generalized plant P is defined as follows:

$$\begin{bmatrix} u_s \\ y_s \\ e \\ \hdashline r_s \\ y_s \end{bmatrix} = \underbrace{\left[\begin{array}{cc:c} 0 & 0 & I \\ M_s^{-1} & 0 & G_s \\ \lambda M_s^{-1} & -\lambda^2 T_r & \lambda G_s \\ \hdashline 0 & \lambda I & 0 \\ M_s^{-1} & 0 & G_s \end{array}\right]}_{P} \begin{bmatrix} w \\ r \\ \hdashline u_s \end{bmatrix} \tag{12}$$

Then P is further calculated as follows:

$$P = \left[\begin{array}{cc|cc:c} A_s & 0 & 0 & Z_c C_s^T & B_s \\ 0 & A_r & B_r & 0 & 0 \\ \hline 0 & 0 & 0 & 0 & I \\ C_s & 0 & 0 & I & 0 \\ \rho C_s & -\rho^2 C_r & 0 & \rho I & 0 \\ \hline 0 & 0 & \rho I & 0 & 0 \\ 0 & 0 & 0 & I & 0 \end{array}\right] = \left[\begin{array}{c|cc} A & B_1 & B_2 \\ \hline C_1 & D_{11} & D_{12} \\ C_2 & D_{21} & D_{22} \end{array}\right] \tag{13}$$

The 2-DOF loop-shaping controller in Fig. 6 can be separated into a state estimator (or observer) and a state feedback controller. According to Walker [13], the state feedback stabilizing controller $K(s)$ satisfying $||F_L(P,K)||_\infty < 1$ has the following realization:

$$K(s): \begin{cases} \dot{\hat{x}}_s = A_s \hat{x}_s + H_s(C_s \hat{x}_s - y_s) + B_s u_s \\ \dot{x}_r = A_r x_r + B_r r \\ u_s = -B_s^T X_{\infty 11} \hat{x}_s - B_s^T X_{\infty 12} x_r \end{cases} \tag{14}$$

where $X_{\infty 11}$ and $X_{\infty 12}$ are elements of

$$X_\infty = \begin{bmatrix} X_{\infty 11} & X_{\infty 12} \\ X_{\infty 21} & X_{\infty 22} \end{bmatrix} \tag{15}$$

In this formulation, $X_\infty \geq 0$ is a solution to the following algebraic Riccati equation:

$$X_\infty A + A^T X_\infty + C_1^T C_1 - \bar{F}^T (\bar{D}^T \bar{J} \bar{D}) \bar{F} = 0 \tag{16}$$

where

$$\bar{F} = (\bar{D}^T \bar{J} \bar{D})^{-1} (\bar{D}^T \bar{J} C + B^T X_\infty) \tag{17}$$

$$\bar{D} = \begin{bmatrix} D_{11} & D_{12} \\ I_w & 0 \end{bmatrix} \tag{18}$$

$$\bar{J} = \begin{bmatrix} I_z & 0 \\ 0 & \gamma^2 I_w \end{bmatrix} \tag{19}$$

Finally, observer or an estimator can be designed to match the values of the state vector of the plant in which the states of many systems cannot be directly observed, and hence state feedback is not possible. The observer-based control system is depicted in Fig. 7.

In this control structure, it is noted that

$$F_s \triangleq B_s^T X_{\infty 11} \tag{20}$$

$$F_r \triangleq B_s^T X_{\infty 12} \tag{21}$$

And the observer is calculated by solving following equation:

$$H_s = -Z_s C_s^T \tag{22}$$

where Z_s is the appropriate solution to the generalized algebraic Riccati equation:

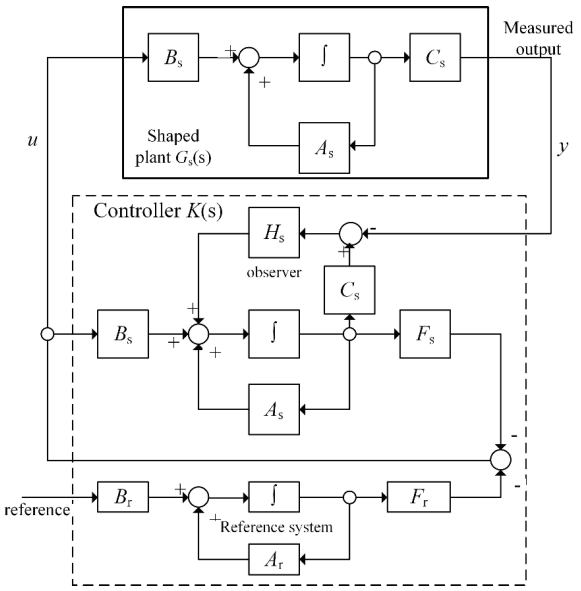

Fig. 7. Control structure of 2-DOF H_∞ loop-shaping.

$$(A - BS^{-1}D^{T}C)Z + Z(A - BS^{-1}D^{T}C)^{T} - ZC^{T}R^{-1}CZ + BS^{-1}B^{T} = 0 \quad (23)$$

With

$$R = I + DD^{T}, \quad S = I + D^{T}D \quad (24)$$

4. Simulation results

In this study, first, the control system regulates the COD concentration of the effluent at 2 g/L. This is a typical value if COD is too low, it needs more control energy and higher COD will be harmful to the surrounding environment. Next, it should estimate the value of VFA in the case of sensor insufficiency. The maintenance and operation of the sensors to measure VFA are very expensive and challenging. Dealing with this difficulty, the robust controller with observer can reduce the cost and complexity for AD system. In addition, it can increase the reliability of the complete system.

Figs. 8 and 9 show the COD concentration under the effect of disturbance and parameter variation. It is known that influent parameter variations and disturbance can deeply affect the effluent COD. The fundamental idea of advanced control strategy is to add external disturbances on purpose on the input flow rate by assuming possible variations of the plant parameters. There are then three possible types of plants: nominal, minimum, and maximum model. First, in order to check the controller's performance, a random disturbance is added to the system as in Fig. 8. This disturbance is trying to drive the COD from its reference. A feedback control system with external disturbance provides corrective action to eliminate the disturbance effects. It can be observed that the COD concentration has only some slight changes due to large disturbances. The control system keeps the COD stable at the desired value, despite the large disturbances. The COD variations are also eliminated whenever the disturbance values are not changing. The control signal shows some actions to bring the COD back to the desired value. The low variations of control output indicate that energy consumption is also low.

Fig. 9 illustrates the time responses of the system regarding the minimum and maximum values of influent COD and VFA as given in Table 1. For the sake of clarification, three models including nominal, minimum, and maximum values were created. The nominal model used the parameter at the linearized point while the minimum and maximum models take the minimum and maximum value of the COD and VFA, respectively. It can be seen that the three models have identical responses. As shown in the lower part of Fig. 9, there is almost no difference between the trajectories. The result proves that the controller can deal with parameter variation effectively. It means whenever influent parameter changes, the controller can adjust dilution rate and retains the coexistence of biomass to regulate the effluent COD at a desired value.

Fig. 10 shows the observer performance on the estimation of VFA state and the detailed estimation at the initial time for clarification. Assuming that the initial value of the real VFA is 30 mmol/L and that of the estimated VFA is 19 mmol/L. It can be noted that the estimated state can track the real state without big difference. After working about 200 h, the estimated error is practically zero with ensuring the perfect tracking. Assume that at 600 h there is a sudden change of the influent from 30 to 200 mmol/L, which describes the maximum perturbed value given in Table1. The VFA estimation is

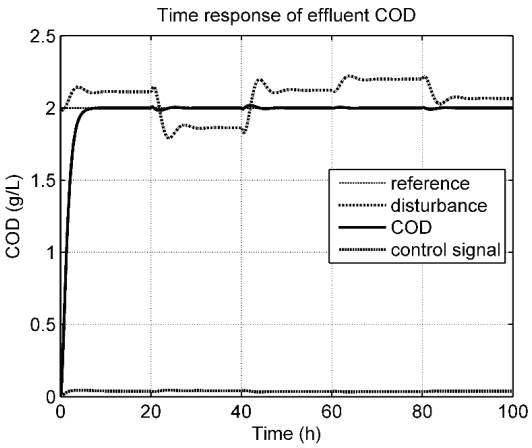

Fig. 8. Time evolutions of COD concentration under disturbances.

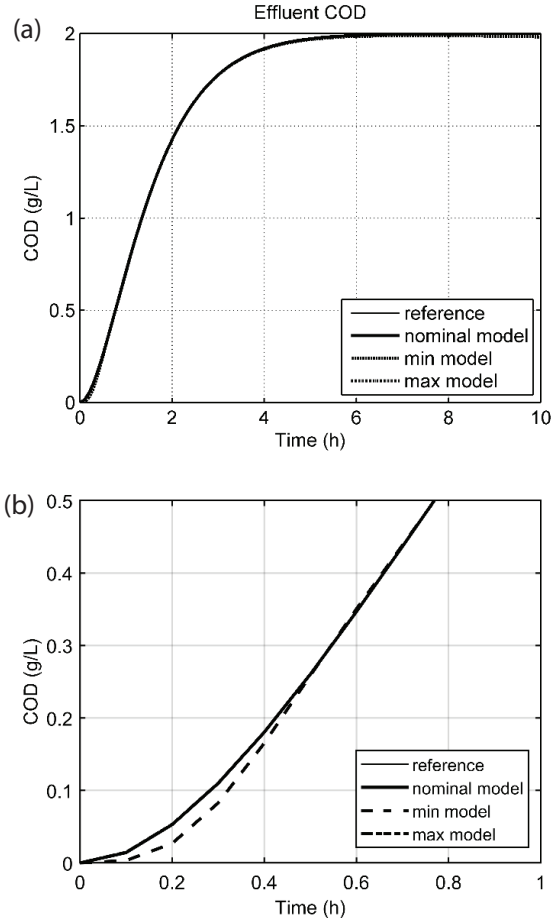

Fig. 9. (a) Time responses of three distinguished models and (b) their detailed illustrations.

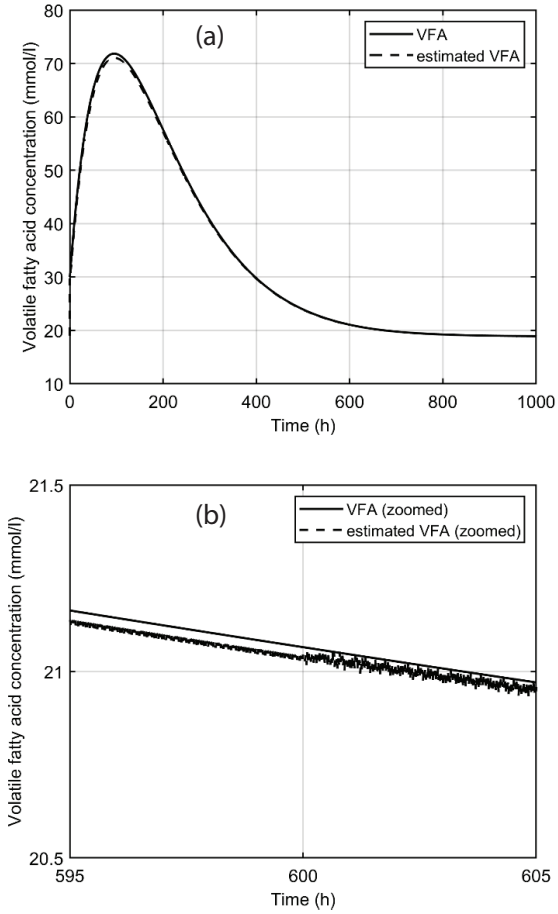

Fig. 10. (a) VFA estimation and (b) its detailed estimation.

magnified for clarify as in the lower part of Fig. 10, showing that there exists variation in the estimated state, but it is still very close to the real one.

Because sensors always have to face the effects of measurement noises, this result suggests that the current observer can be an ideal replacement for VFA sensor. It can not only perfectly estimate the state values, but can also not affected by sensor noises. The VFA estimation by observer may provide useful information for monitoring and controlling the complete system, when one can not measure all state variables often the case in practice. For example, the monitoring system can trigger some tasks when VFA concentration reaches a certain level.

5. Conclusions

The controlling and monitoring systems in the AD process have been facing difficulties due to internal uncertainties, external disturbances, and sensor noises. The difficulties are also expressed by means of nonlinear analysis. By using the coprime uncertainty, the control system accounted for any kind of uncertainty that can exist in an AD system. The loop-shaping procedure allows designers to shape the system as desired. The 2-DOF controller gives flexibility in the robustness satisfaction and reference tracking. The simulation results show that the controller successfully deals with parameter uncertainties as well as disturbances. Furthermore, this observer-type robust control can exactly predict some system states, specifically, VFA in the case where there is no such sensor. The above performances prove that the observer-based H_∞ loop-shaping controller is very active. Based on this control configuration, the COD can be robustly regulated and the VFA value can be exactly estimated, overcoming the limitation of difficulty in the implementation of complex and expensive sensors or analysers. This algorithm gives some potential solutions for the development of modern AD systems.

References

[1] D. Gaida, C. Wolf, M. Bongards, Feed control of anaerobic digestion processes for renewable energy production: a review, Renewable Sustainable Energy Rev., 68 (2016) 869–875.
[2] R.A. Flores-Estrella, G.Q. Compean, H.O. Mendez-Acosta, R. Femat, H∞ control of anaerobic digester for winery industry wastewater treatment, Ind. Eng. Chem. Res., 52 (2013) 2625–2632.
[3] H. Spanjers, J.B.V. Lier, Instrumentation in anaerobic treatment – research and practice, Water Sci. Technol., 53 (2006) 63–76.
[4] J.P. Steyer, O. Bernard, D.J. Batstone, I. Angelidaki, Lessons learnt from 15 years of ICA in anaerobic digesters, Water. Sci. Technol., 53 (2006) 25–33.
[5] H.O. Mendez-Acosta, B. Palacios-Ruiz, V. Alcaraz-Gonzalez, V. Gonzalez-Alvarez, J.P. Garcia-Sandoval, A robust control scheme to improve the stability of anaerobic digestion processes. Comput. Chem. Eng., 20 (2010) 375–383.
[6] D.T. Hill, Simplified monod kinetics of methane fermentation of animal wastes, Agric. Wastes, 5 (1983) 1–16.
[7] O. Bernard, Z. Hadj-Sadok, D. Dochain, A. Genovesi, I.P. Steyer, Dynamical model development and parameter identification for an anaerobic wastewater treatment process, Biotechnol. Bioeng., 75 (2001) 424–438.
[8] D.J. Batstone, J. Keller, I. Angelidaki, S.G. Pavlostathis, A. Rozzi, W.T. Sanders, H. Siegrist, V.A. Vavilin, Anaerobic Digestion Model No.1 (ADM1), 1st ed., IWA Publishing, London, 2002.
[9] H. Siegrist, D. Vogt, J.L. Garcia-Heras, W. Gujer, Mathematical model for meso- and thermophilic anaerobic sewage sludge digestion, Environ. Sci. Technol., 36 (2002) 1113–1123.
[10] M. Sbarciog, M. Loccufier, E. Noldus, Determination of appropriate operating strategies for anaerobic digestion systems, Biochem. Eng. J., 51 (2010) 180–188.
[11] D. McFarlane, K. Glover, A loop-shaping design procedure using H∞ synthesis, IEEE Trans. Autom. Control, 37 (1992) 759–769.
[12] D.J. Hoyle, R.A. Hyde, D.J.N. Limebeer, An H∞ Approach to Two Degree of Freedom Design, Proc. 30th Conference of Decision and Control, Brighton, UK, 1991.
[13] D.J. Walker, On the structure of a two-degree-of-freedom H∞ loop shaping controller, Int. J. Control, 63 (1996) 1105–1127.

Appendix A

$$A = \begin{bmatrix} 0 & 0 & 0.003 & 0 \\ 0 & 0 & 0 & 0.077 \\ -0.421 & 0 & -0.148 & 0 \\ 1.165 & -2.68 & 0.354 & -20.785 \end{bmatrix} \quad \text{(A1)}$$

$$B = \begin{bmatrix} -0.337 \\ -25.912 \\ 14.22 \\ 64.32 \end{bmatrix} \quad \text{(A2)}$$

$$C = \begin{bmatrix} 0 & 0 & 1 & 0 \end{bmatrix} \quad \text{(A3)}$$

$$D = \begin{bmatrix} 0 \end{bmatrix} \quad \text{(A4)}$$

$$G = \frac{14.23s + 0.142}{s^2 + 0.148s + 0.00128} \quad \text{(A5)}$$